CHAPTER 3

THE ZEUS EXPERIMENT AT HERA

In experimental high energy physics researches, the particle accelerator provides a high precision instrument for the scientist to conduct research on structure of elementary constituents of matter and the interaction of radiation with matter to understand the basic building blocks that made up the universe. Particle collider such as Hadron-Elektron Ring Anlage (HERA) at Deutsches Electronen Synchrotron (DESY) was one of the pioneers in experimental high energy physics to study the mechanism of hadrons being bound within the nucleus. The ZEUS detector at HERA was constructed as a powerful and versatile detector to measure particles and jets production with energies up to several hundred GeV.

3.1 The HERA Storage Ring

Deutsches Electronen Synchrotron (DESY) was founded in 1959 and part of Helmholz Association, is dedicated to fundamental research in particle physics and the study of synchrotron radiation. DESY at Hamburg campus is home to several particle accelerators, namely DESY accelerator, the linear accelerator (LINAC) the Positron-Elektron Tandem Ring Anlage (PETRA), the Doppel Ring Speicher (DORIS), and the Hadron-Elektron Ring Anlage (HERA) [5].

HERA began its operation in 1992, was the first electron-proton collider in the world to study the scattering interactions between electron of 30 GeV and protons of 920GeV. With circumference 6.3km, HERA two-ring accelerator s located between 10 m and 25 m deep underground (see Figure 3.1).

The protons from the negatively charged hydrogen (H^-) ions were accelerated in phases from 50 MeV in LINAC after which the beam were stripped of the electrons when it passed through a thin foil, to 7.5 GeV in PETRA and accelerated up to 39 GeV before being injected into the HERA ring. In HERA ring, the superconducting dipole magnet with file strength of 4.65 T accelerated the proton further up to 920GeV before it reached the ZEUS detector [5].

The electron and positron for lepton beams at HERA were obtained from the e^+e^- pair production from the bremsstrahlung process of the tungsten sheet. The electron beam were accelerated to 7GeV before being fed into PETRA II, and finally being accelerated up to 27.5GeV by the 0.165 T dipole magnets in the HERA ring before it reached the ZEUS detector.

In the ZEUS detector, the 920GeV proton beam and the 27.5GeV electron beam collided head on to produce leptons, new quarks, hadrons, neutrinos, photons etc., where the data observed during the physics events were recorded by the a an on-line readout control and kept in the DESY data storage system for event reconstruction later.

During the physics experiment, Monte Carlo event generators could be triggered to simulate the physics event simultaneously – these Monte Carlo data would be kept together with the on-line data from the physics experiments in the DESY data storage system for analysis together with the event reconstruction later.

Figure 3.1a HERA and PETRA accelerators aerial view at the DESY campus in Hamburg, HERA is at 10 - 20m underground with circumference 6.3km.

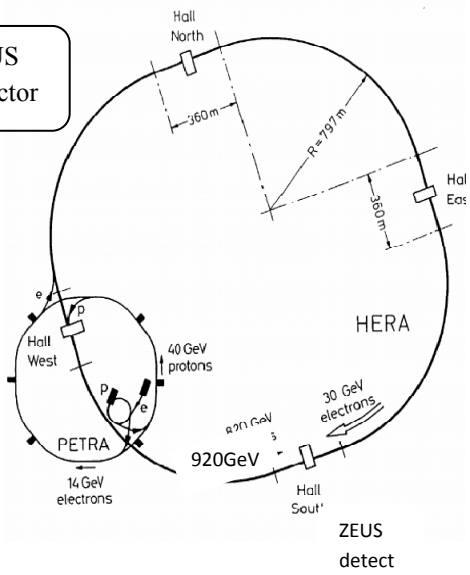

3.1b Schematic diagram of the HERA layout with ZEUS detector at south of HERA

3.2 The ZEUS Detector

The ZEUS detector, located 30 m underground at the southern of HERA experimental hall, was a powerful and versatile detector dedicated to experimental high energy physics, to probe the electron and quark substructure to distance of a few $10^{-18}\,cm$ and search for new mediators of neutral and charge currents phenomena during the electron-proton beam collision at the centre of the ZEUS detector. In **Figure 3.2**, the longitidunal layout of the ZEUS detector is given [41]. The ZEUS detector comprised of the following components:

(i) vertex detector (VTX)

(ii) central tracking detector (CTD), in the field of a thin magnetic solenoid

(iii) a transition radiation detector (TRD)

(iv) a planar drift chambers (FTD,RTD)

(v) an electromagnetic calorimeter (EMC)

(vi) a hadronic calorimeter (HAC) surrounding full solid angle over the solenoid

(vii) a backing calorimeter (BAC)

(viii) a barrel and rear muon detector (MU)

(ix) a forward muon spectrometer (FMU)

(x) hadron electron separator (HES)

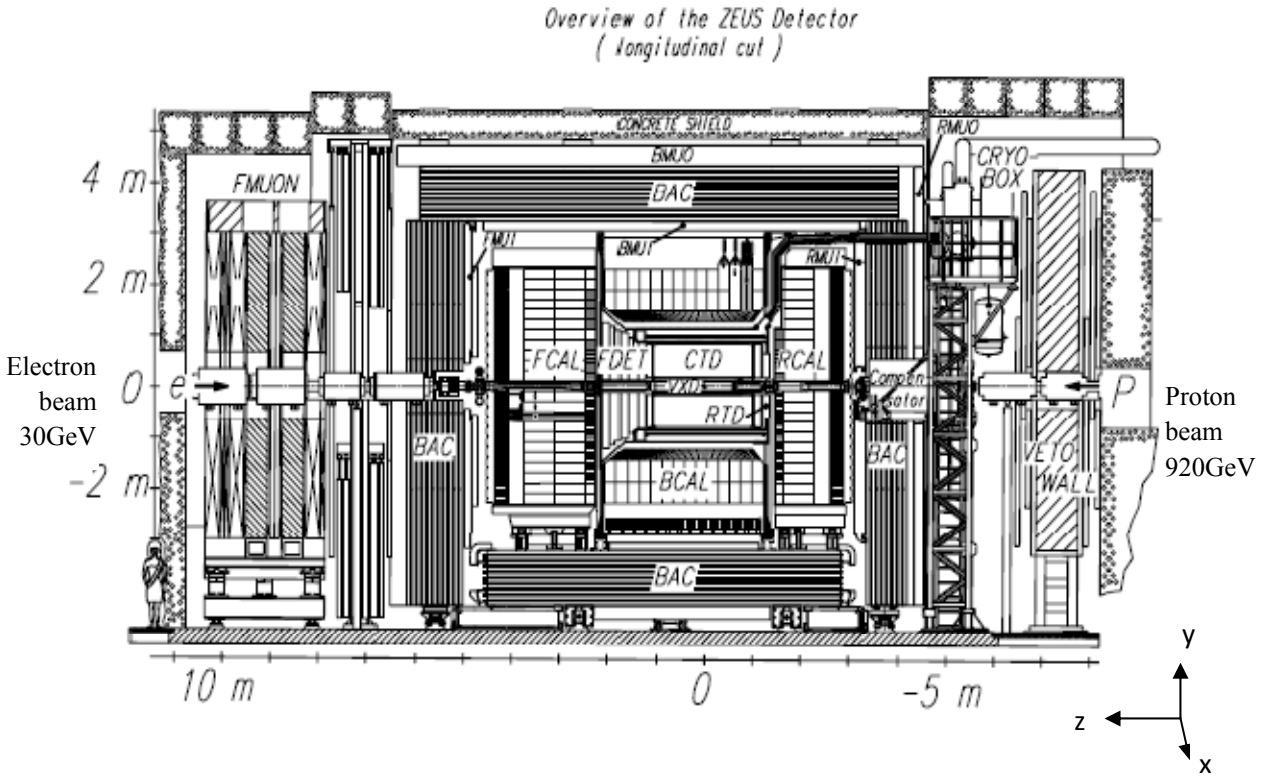

Figure 3.2 Longitudinal cross section view of the Zeus detector [41]. The FCAL, BCAL and the RCAL forms the hadronic calorimeter of the ZEUS detector

3.2.1 The High Resolution Calorimeter

The calorimeter of the ZEUS detector was designed for high energy resolution, uniformity, stability and fast response with the ability to handle up to 10.4MHz of HERA bunch crossing rate. The hadronic energy resolution of the calorimeter was $\sigma(E)/E = 0.35/\sqrt{E} \oplus 2\%$ E in GeV, ($\oplus$ stands for addition in quadrature), while the electromagnetic energy resolution was $\sigma(E)/E = 0.18/\sqrt{E} \oplus 1\%$ [41]. The three main regions of the detector were the forward (FCAL), the barrel (BCAL) and the rear (RCAL). Each region was subdivided into small modules and consist of towers segmented into two parts i.e. the inner parts that constitutes electromagnetic section

(EMC) that detect electromagnetic showers, while the outer parts constitutes the hadronic section (HAC) that detects the hadronic showers. **Figure 3.3** shows the schematic of one such module in the ZEUS detector.

3.2.2 The Uranium-Scintilllator

Throughout the modules in calorimeter, thousands of uranium-scintilllator (SCSN-38) plates were sandwiched together to provide signals to the photomultiplier tube (see **Figure 3.3**). The SCSN-38 scintillator, as active material that contained large fraction of hydrogen atoms, produced the signals by interacting with the slow neutrons from the hadronic shower. The wavelength shifter WLS (Y-7 in PMMA) shifted the wavelength of light emitted by scintillator into visible light before being transmitted to the photomultiplier tube (PMT) as signal from the hadrons as it deposited its energy in the CAL.

Uranium, as passive material, produced slow neutrons through fission reaction that helped in compensating losses in the hadronic shower. It also acts as absorber of electromagnetic particle generated in the electromagnetic part of the hadronic shower, thus enhancing the compensation mechanism [42].

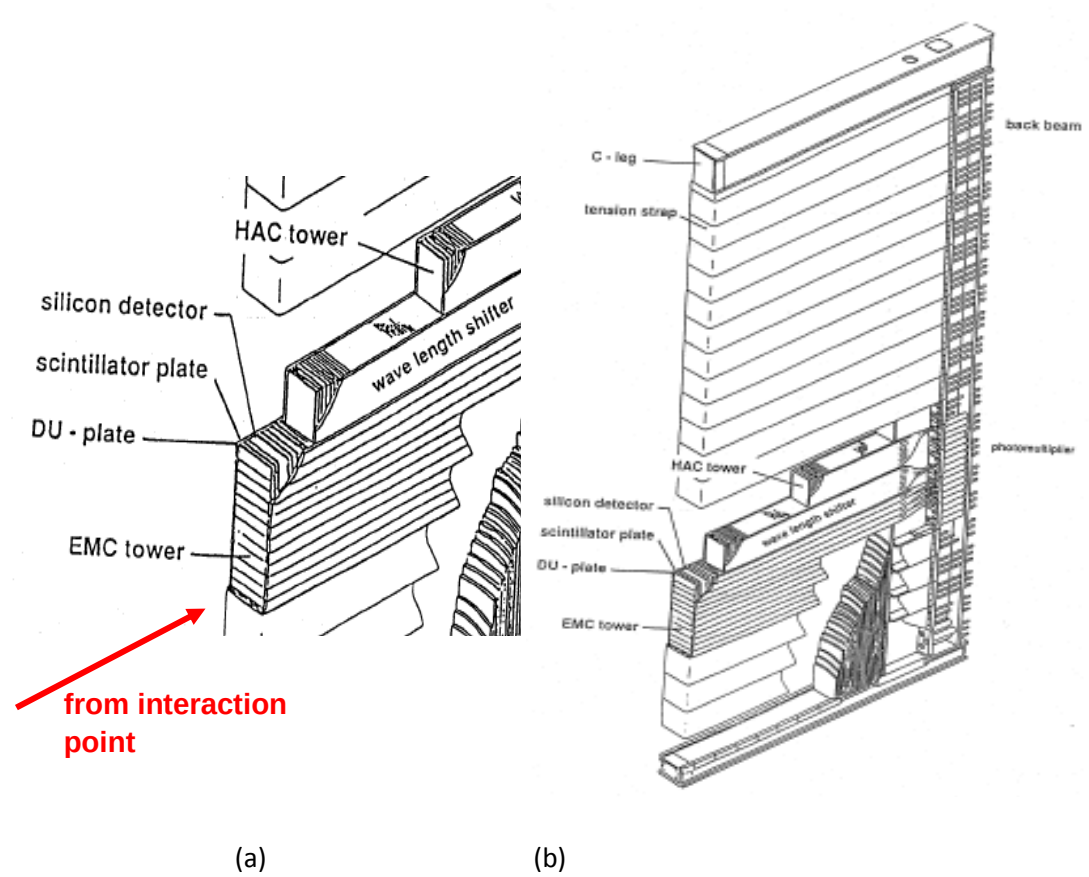

(a) (b)

Figure 3.3 (a) Structure of a tower in a module of a Forward Calorimeter (FCAL) showing the uranium-scintillator sandwich; (b) Side view of a FCAL module . The uranium as passive material produced slow neutron to compensate losses of hadronic shower, while act as absorber to electromagnetic particles. The active scintillator SCSN-38 interacts with slow neutrons from hadronic shower to produce signals for photomultiplier tube (PMT) via the wavelength shifter (WLS) [42][43]

3.2.3 Calorimeter Layout

Figure 3.2 shows the calorimeter which consist of forward hadronic calorimeter (FCAL) and forward electromagnetic calorimeter (FEMC) at the front-end of the calorimeter, the barrel calorimeter (BCAL) and the barrel electromagnetic calorimeter (BEMC) surrounding the middle part of the calorimeter, and the rear calorimeter (RCAL) and rear electromagnetic calorimeter (REMC) at the rear-end, with properties as given in

Table 3.3. BCAL and FHAC comprised of two layers BHAC1 and BHAC2, FHAC1 and FHAC2 respectively, while RHAC consist of only one layer.

During the electron-proton collision, the particles during the interaction would either travel from the point of interaction right to the outer layer of the detector. The particles of electromagnetic radiation such as photons and electrons, traveled from the interaction point at the centre of the detector hitting the superlayers in the central tracking detector (CTD) to the electromagnetic calorimeters BEMC, FEMC and REMC and deposited 95% of its energy there. The hadrons, on the other hand, would deposit 30% of its energy at the electromagnetic calorimeters [3], and continue their paths to the hadronic calorimeters BHACs, FHACs and RHAC.

These particles moved through the uranium-scintilllator sandwich to provide optical signals to the photomultiplier tubes and then to the readout control of the ZEUS detector. **Figure 3.4** shows the showering pattern of the electromagnetic, hadrons and muon showers with the muons having highest penetration depth. Halomuons produced during the proton beam injection into the ZEUS detector, moved in straight path from the rear to the forward calorimeter without losing much of their energies.

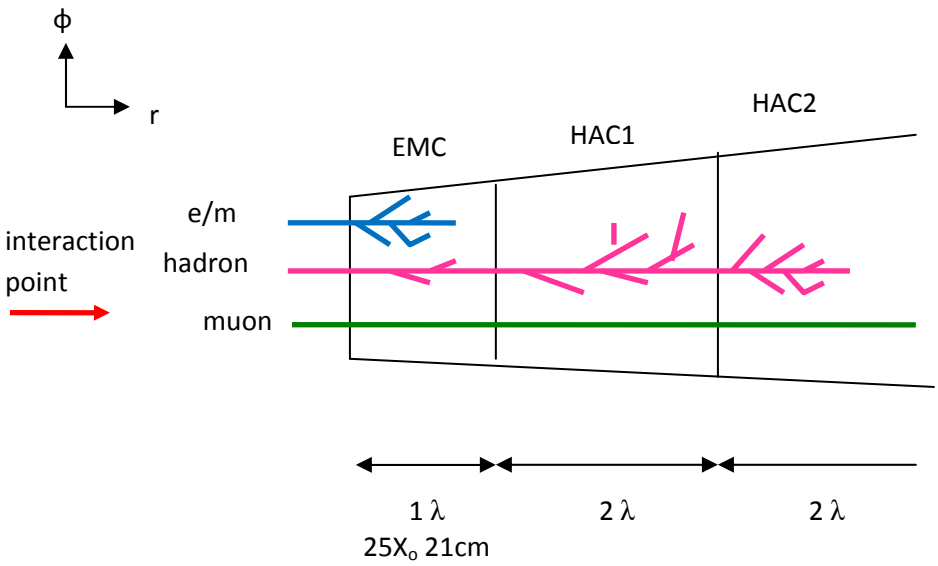

Figure 3.4 Diagram of BCAL tower, with EMC cells backed 2 HAC cells (BCAL towers were projective in η and θ). The hadron particles, electromagnetic (e/m) particles and mouns shower differently in the calorimeter

Table 3.1 Properties of ZEUS CAL listed by section

	FCAL	BCAL	RCAL
Angular coverage (θ)	2.2^0 to 39.9^0	36.7^0 to 129.1^0	128.1^0 to 176.3^0
Angular coverage (η)	101 to 3.95	-0.74 to 1.10	-3.90 to - 0.72
Number of modules	24	32	24
Towers/Modules	11 to 23	16	11 to 23
Number of cells	2172	2592	1668
Depth (m)	1.5	1.07	0.84
Depth (λ)	7.1	5.1	4.0
Depth (X_0)	181.0	129.0	103.0
EMC Front Face Dimension (cm)	5 x 20	5 x 20	10 x 20

3.2.4 ZEUS Tracking Detector

In the ZEUS detector, the trajectory of charge particles such as $\pi^{\pm}, \mu^{\pm}, e^{\pm}, p$ were tracked by the ZEUS tracking detector that comprised of Central Tracking Detector (CTD) and the vertex detector (VTX). In **Figure 3.2,** the CTD is located at the centre ZEUS detector surrounding the vertex detector (VTX).

With active volume 202.4cm between endplates and radial coverage between *r*=19.0cm(innermost) and *r* =78.5cm(outermost), the inner volume of the CTD was lined with 9 superlayers – each superlayers consist of a matrix of 3905 sense wire referred to as cells. When a charge particle passed through the superlayers and hitting the sense wires, the drift distance were digitized. Charge particles produced during the electron-proton-collision and hitting the sense wire inside the CTD would be deflected from its origin.

With an axial magnetic field of 1.8T and radial force distribution along the coil axis of the magnetic field in the CTD of $\int_{-120}^{130} F_r dz = 661\, tons$ supplied by superconducting solenoid between the CTD and barrel calorimeter, the charged particles were deflected for momentum measurements. **Figure 3.5** gives the helix of a CTD hit, where ϕ is the outbound tangent angle in XY plane and, θ as the angle of dip with regard to the XY plane, with the reconstructed momentum as [46],

$$\left(p_x, p_y, p_z\right) = \left(p\cos\phi\sin\theta, p\sin\phi\sin\theta, p\cos\theta\right) \qquad (3.1)$$

Inside the coil, the magnetic field is approximately parallel to the Z-axis. At any point of a track's trajectory, the path is approximately as an axial helix.

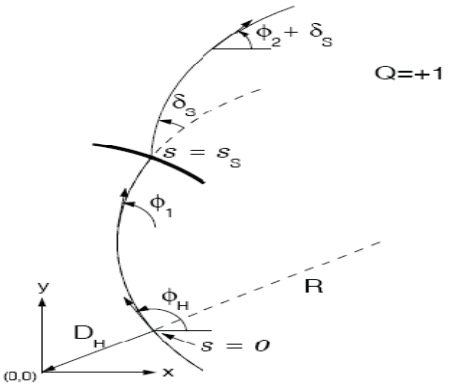

Figure 3.5 A helix in XY plane, where ϕ is the outbound tangent angle in XY plane in the CTD [46]

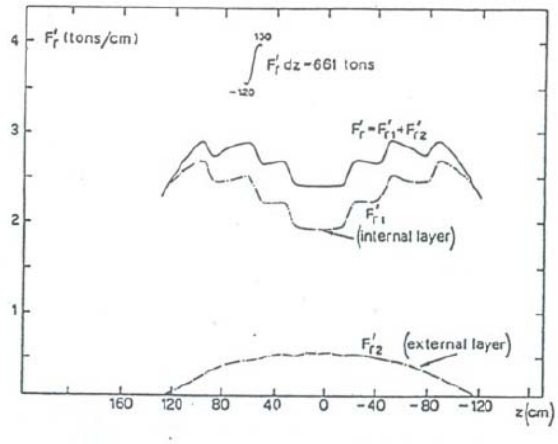

Figure 3.6 Radial force distribution along the coil axis of the magnetic field in central tracking detector (CTD) [41]

Table 3.2 Centre radius of superlayers in the CTD of ZEUS detector [1]

Superlayer	Centre radius of cell (cm)
1	20.97
3	35.00
5	48.73
7	62.74
9	76.54

Figure 3.7 CTD layout of the ZEUS detector [1]

3.2.5 Hadron Electron Separator (HES)

In the ZEUS detector, the Hadron Electron Separator (HES) was used to differentiate electromagnetic showers (electrons) from hadronic showers, to provide the researchers with complimentary data of the electron-proton collision, especially on the electrons from the charm quark decay and to differentiate it from photon showers from electron-proton collision.

Located at the inner front of part of the front and rear calorimeter **(Figure 3.8),** the silicon pad detector on HES recorded the energy deposited by the electron as it passed through the detector. As each the dimension of cell on the pad silicon smaller (3cm x 3cm) than the cell on the calorimeter (20cm x 20cm) the resolution of the electron signal from HES was more refined than the calorimeter. **Figure 3.9** shows the arrays of cells in the calorimeter with silicon pads mounted across the calorimeter.

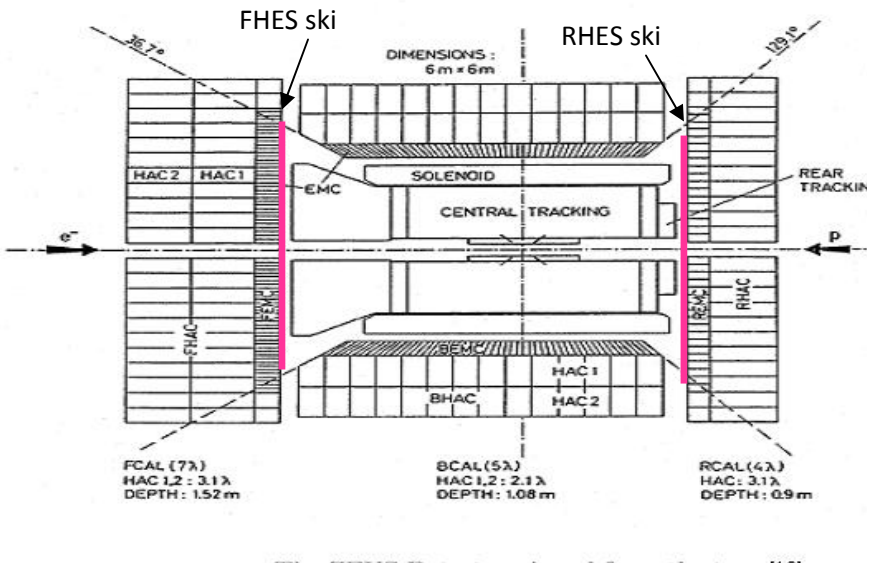

Figure 3.8 Front and rear Hadron Electron Separator (HES) FHES and RHES respectively, in front of calorimeter in the ZEUS detector

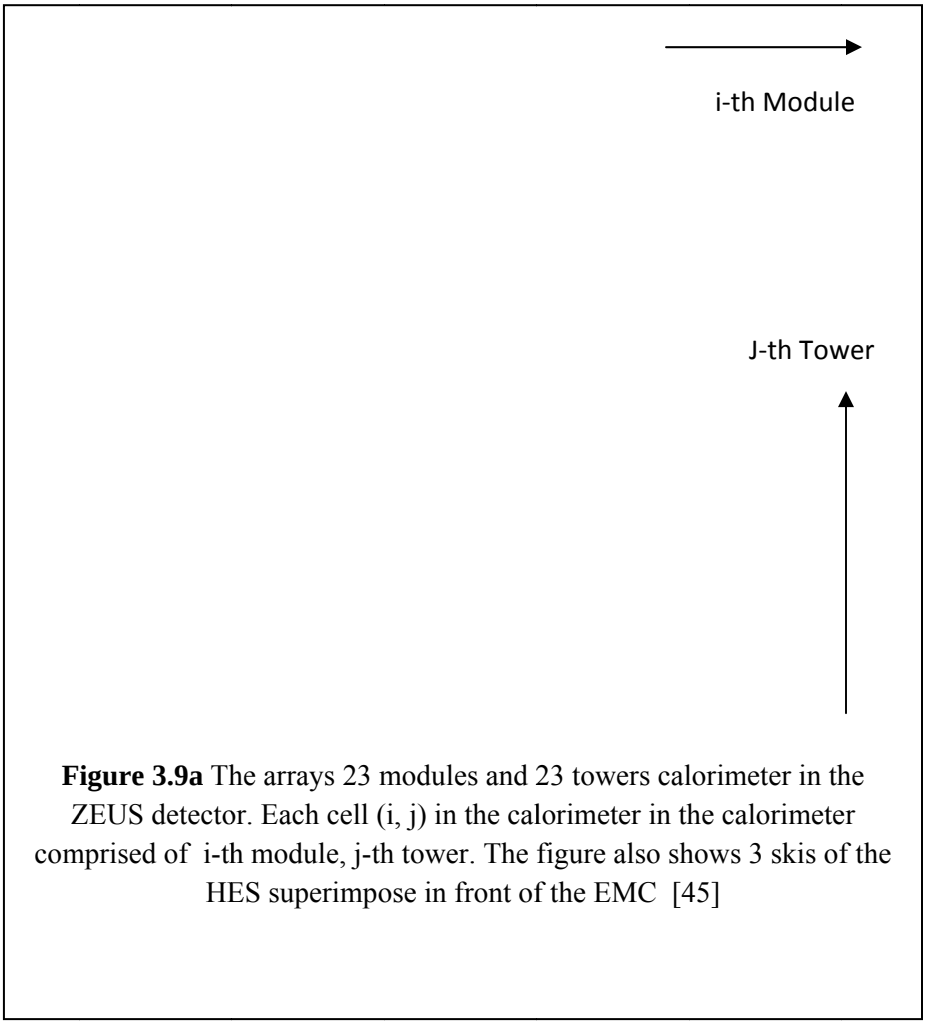

Figure 3.9a The arrays 23 modules and 23 towers calorimeter in the ZEUS detector. Each cell (i, j) in the calorimeter in the calorimeter comprised of i-th module, j-th tower. The figure also shows 3 skis of the HES superimpose in front of the EMC [45]

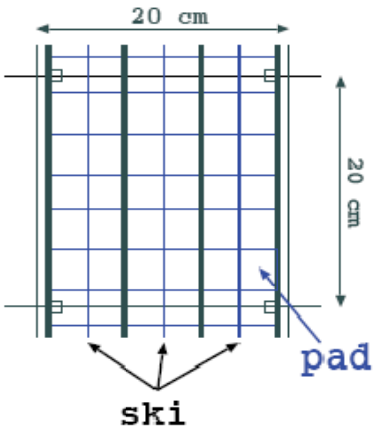

Figure 3.9b Silicon pad (3cmx3cm) mounted on skis, map to one calorimeter cells [45]

3.3 Calorimeter Tracking and ZUFOS

In the calorimeter of the ZEUS detector, the particles originated from the electron-proton collision traveled the across the detector to the calorimeter to deposit its energy in the calorimeter. The energy deposits by hadrons in the final states (whether charge or neutral) and the electromagnetic showers, were recorded by each cells in the calorimeter. **Figure 3.10** shows the trajectory of neutral and charge particles arriving at the calorimeter in the ZEUS detector and depositing energy in the calorimeter cells.

In tracking the particles passing through the calorimeter, each cell of the calorimeter containing energy deposits were clusters to form cone islands, resulting in three dimensional objects known as ZEUS Unidentified Flow Objects (ZUFOs).

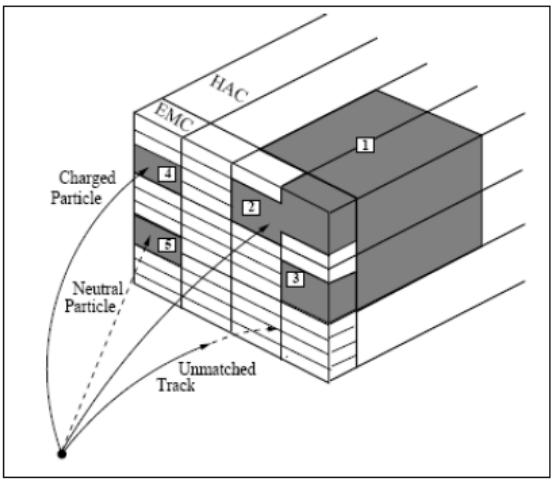

Figure 3.10 Neutral ZUFOs move in straight trajectory from the interaction point through the EMC (electromagnetic calorimeter) to HACs (hadronic calorimeters) in the ZEUS detector, forming islands of energy deposits in the calorimeter. Neighboring cells were clustered to form cone clusters and matched to tracks [2].

These ZUFOs tracks were fitted to the primary vertex. Good tracks were selected if the distance of closest approach (DCA) between extrapolated track from inner surface of calorimeter to the associated island was less than 20cm, or DCA was less than the maximum radius from the plane perpendicular to a ray drawn from the vertex to the island [2].

The energy of charged ZUFOs was determined from the four-momenta by assuming the particle as a pion. The neutral energy of ZUFOs was selected if it was not associated with any track. In this thesis, the ZUFOs were selected as potential candidates for long-lived neutral hadrons in the final states.

3.4 Monte Carlo Event Simulation

To compare the experimental results against theoretical model, the on-line ZEUS detector was equipped with Monte Carlo simulations. **Figure 3.11** gives the flow diagram of the simulation in the ZEUS detector that was being run concurrent to the physics event during electron proton collision.

In the Monte Carlo simulation environment for ZEUS, MOZART (Monte Carlo for ZEUS Analysis, Reconstruction and Trigger), which used the GEANT package, to simulate passage of particles passing the geometry and materials in the ZEUS detector. After MOZART, the event was processed by CZAR (Complete ZGANA Analysis Routine) that simulated ZEUS on-line trigger components based on test beam parameters [5].

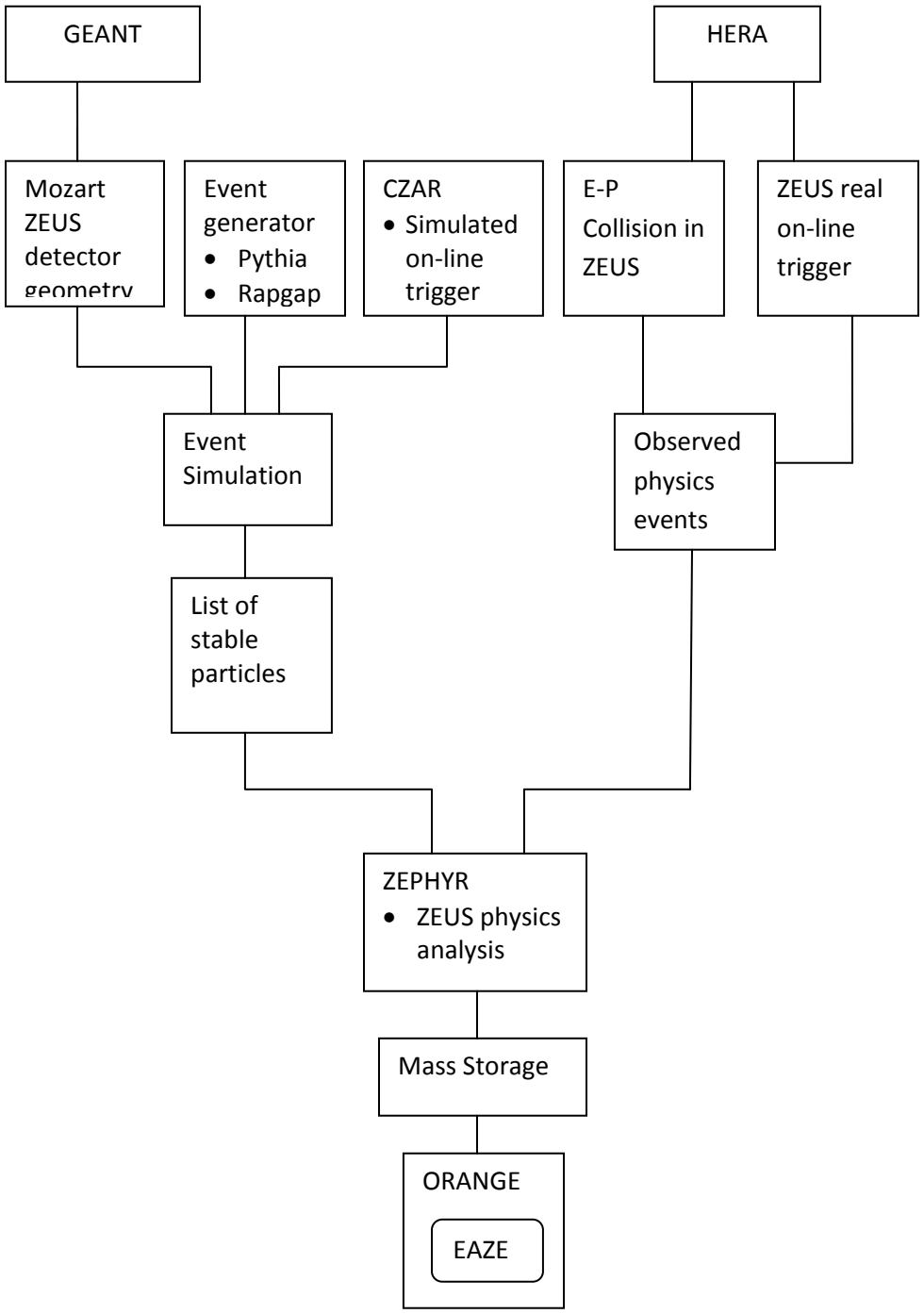

Figure 3.11 Flow diagram of event analysis in the ZEUS detector. Simulated and actual events were run concurrent and compared to extract correction factor from pQCD calculation.

Event generator such as Pythia, Rapgap, Ariadne, Djanggoh were used to provide sets of outgoing particles produced in the interaction between two incoming particles in the electron-proton collision. During real time operation of the ZEUS detector, the global trigger system of HERA provided inputs to the ZEUS detector that accepted 96ns of HERA clock for its synchronized data taking events.

The actual events from the electron-proton collisions and the simulated events were then passed through ZEUS Physics Reconstruction (ZEPHYR) which applied reconstruction code and calibration constants to the events. The raw data were then stored in tabulated forms on ZEUS Adamo table, and kept on mass storage tape for off-line data analysis, available through EAZE (Easy Analysis of ZEUS Events) program integrated in the Orange (Overlying Routine for Analysis Ntuple Generation) package.

3.4.1 Event Generators

The objective of event generators is to use computers to generate events with the same average behavior and the same fluctuation as real data, as detailed as could be observed by a perfect detector by 'factoring' full problems into a reasonably accurate components, with objects branching into two which daughters were free to branch themselves. Monte Carlo technique was used to select all relevant variables based on probability distribution in the final events [48].

The complexity of high energy physics process that based on the level of interactions between fundamental objects i.e. quarks, leptons and gauge bosons , using 'skeleton' process $e^+e^- \to Z^0 \to q\bar{q}$ that branched into subprocesses $e \to e\gamma$ or $q \to qg$, could be treated as 'parton showers' where one initial parton may branched into a whole bunch of

partons in the final states, coupling constant α_s that determined the momentum transfer of scale in the parton showering process.

In case of quark and gluon, the structure of incoming hadrons and the hidronisation process, where colored partons (quark and gluons) transformed themselves into colorless hadrons, photons and leptons, fragmentations and decays might take place. These subprocesses were based on specific models such as Lund string model or Color Dipole Moment (CDM).

3.4.1.1 Pythia

In Pythia, the hard process of $e^+e^- \to \gamma^* / Z^0 \to q\bar{q}$, with virtual photon γ^* from of the mass shell, the final state quark *q* might be *u*, *d*, *s*, *b* or *t*, with the flavor picked at random according to the relative couplings evaluated at the hadronic centre of mass (c.m.) energy [48].

In the tunneling picture of the Lund string model, the suppression of heavy-quark production to a ratio $u : d : s : c \approx 1 : 1 : 0.3 : 10^{-11}$ implied that charm and heavier quarks were not expected to be produced in soft fragmentation, but in perturbative parton-shower branching $g \to q\bar{q}$.

When quark-antiquark $q\bar{q}$ pair from two adjacent string moved apart to form a meson, notably a pseudoscalar or vector meson, a quantitative ratio of 1:3 from counting the number of spin states was expected, with the color flow not always well-defined – an algorithm was need to choose between the two.

In the fragmentation process, a large fraction of unstable particles produced decayed into observable stable ones, assuming that the decay products were distributed to phase

space with no dynamics involved, where branching ratios and decay modes in normal decay treatment were used.

In baryons production, diquark in antitriplet state behaved as an ordinary antiquark, such that a string could break either by quark-antiquark or antidiquark-diquark pair production (which was not well represented).

3.4.1.2 Ariadne

In simulating the QCD cascade, Ariadne uses the Color Dipole Moment (CDM) to generate particles in e^+e^- and lepton-hadron experiments using the coherence effects in the gluon bremsstrahlung for radiation between two color dipoles as described in **Section 2.7** of **Chapter 2**.

As one of the "Lund family Monte Carlo programmes", Ariadne only generates the QCD cascade process and is commonly interfaced with other programmes such as PYTHIA, JETSET and LEPTO that handle hard interactions, hidronisation and particle decays.

In approximating the CDM interactions during a $q\bar{q}$ splitting, ordering of transverse momentum $p_\perp$ in the phase space was applied i.e. $p_{\perp 1} > p_{\perp 2} > p_{\perp 3} > .p_{\perp i} > ...$ where i=1,2, 3 … refers to the first, second, third dipole originally generated from the first $q\bar{q}$ pair. In case of qg dipole splitting, the gluon always retain its original directing when the color flow in the neighboring dipoles is minimized while the gg dipole is distributed as given by **Equation (2.7)** in **Chapter 2** of this thesis.